FEBS Letters 588 (2014) 2003–2008

journal homepage: www.FEBSLetters.org

Site-specific phosphorylation of Tau protein is associated with deacetylation of microtubules in mouse spermatogenic cells during meiosis

Hiroki Inoue [a], Yuuki Hiradate [a], Yoshiki Shirakata [a], Kenta Kanai [b], Keita Kosaka [b], Aina Gotoh [b], Yasuhiro Fukuda [c], Yutaka Nakai [c], Takafumi Uchida [b], Eimei Sato [d], Kentaro Tanemura [a,*]

[a] Laboratory of Animal Reproduction and Development, Graduate School of Agricultural Science, Tohoku University, 1-1 Tsutsumidori-Amamiyamachi, Aobaku, Sendai 981-8555, Japan
[b] Molecular Enzymology, Department of Molecular Cell Science, Tohoku University, 1-1 Tsutsumidori-Amamiyamachi, Aobaku, Sendai 981-8555, Japan
[c] Laboratory of Sustainable Environmental Biology, Graduate School of Agricultural Science, Tohoku University, 232-3 Yomogida, Naruko-onsen, Osaki, Miyagi 989-6711, Japan
[d] National Livestock Breeding, 1 Odakurahara, Odakura, Nishigo-mura, Nishishirakawa-gun, Fukushima 961-8511, Japan

ARTICLE INFO

Article history:
Received 12 February 2014
Revised 26 March 2014
Accepted 10 April 2014
Available online 24 April 2014

Edited by Jesus Avila

Keywords:
Meiosis
Spermatogenesis
Testis
Tau

ABSTRACT

Tau is one of the microtubule-associated proteins and a major component of paired helical filaments, a hallmark of Alzheimer's disease. Its expression has also been indicated in the testis. However, its function and modification in the testis have not been established. Here, we analyzed the dynamics of phosphorylation patterns during spermatogenesis. The expression of Tau protein and its phosphorylation were shown in the mouse testis. Immunohistochemistry revealed that the phosphorylation was strongly detected during meiosis. Correspondingly, the expression of acetylated tubulin was inversely weakened during meiosis. These results suggest that phosphorylation of Tau protein contributes to spermatogenesis, especially in meiosis.

1. Introduction

The seminiferous epithelium of the mammalian testis possesses a variety of microtubule networks: an ordered array in Sertoli cells [1], the manchette, axonemal microtubules and in mitotic and meiotic spindles. These abundant microtubule networks are reflected by a diversity of microtubule-associated proteins (MAPs). Therefore, the testis can be a rich source for studies of microtubules and MAPs.

The tau (tubulin-associated unit) protein was identified in 1975 as a protein with the ability to induce microtubule formation [2,3]. Normally, tau is associated with microtubules and promotes their polymerization [3] and stabilization [4,5] depending on its phosphorylation status. For example, highly phosphorylated tau, which is observed in the brains of subjects with Alzheimer's disease (AD), composes paired helical filaments (PHFs) and barely promotes microtubule polymerization [6]. In the central nervous system, alternative splicing of the tau primary transcript generates six isoforms of 352–441 amino acids with an apparent molecular weight of 48–67 kDa [7–9]. Among the 85 putative phosphorylation sites on tau, 45 are serines, 35 are threonines and only 5 are tyrosines [10–12]. Tau is subdivided into four regions: an acidic region in the *N*-terminal part, a proline-rich region, a region responsible for binding with microtubules (microtubule-binding domains), and a *C*-terminal region. Serine phosphorylation at KXGS motifs, belonging to the microtubule-binding domain, decreases tau affinity for microtubules and consequently prevents binding to them [13–15]. Because more phosphorylated tau protein at Thr181, Ser199 and Thr231, belonging to the proline-rich region, is contained in the cerebrospinal fluid of brains from people with AD than in normal brains, it is useful as a biomarker of AD [16–18].

Although tau expression in the testis has been indicated [9,19], its expression and post-translational modification patterns including phosphorylation are barely known for this organ. In rat testis, tau was detected as two major bands with molecular masses of 34 and 37 kDa, and it has been suggested that tau is highly phosphorylated [9]. Phosphorylation, as mentioned above, is one of the most important post-translational modifications. To help elucidate the mechanisms of its function, we analyzed the dynamics of

* Corresponding author. Fax: +81 22 717 8686.
E-mail address: kentaro@m.tohoku.ac.jp (K. Tanemura).

http://dx.doi.org/10.1016/j.febslet.2014.04.021

tau protein expression and post-translational modification, especially phosphorylation, during mouse spermatogenesis.

2. Materials and methods

2.1. Animals

Male C57BL/6 mice at 12 weeks of age were used. All mice were anesthetized with 2, 2, 2-tribromoethanol and perfused with a physiological salt solution before being used for tissue collection. Care and use of the mice conformed to the Regulations for Animal Experiments and Related Activities at Tohoku University.

2.2. Antibodies

Several well-characterized antibodies to phosphorylated tau were used to investigate the level and phosphorylation states of tau protein in the testis. These antibody targets included mouse monoclonal antibody Ms X tau-1 [20] (#MAB3420, Lot: LV1478875, Chemicon), rabbit polyclonal antibody anti-phosphorylated tau^{S199,S202} (p-tau^{S199,S202}) [21] (#54963, Lot: HB131, AnaSpec) and mouse monoclonal antibodies, AT8 [22] (#MN1020, Lot: NG173165, Thermo Fisher Scientific), AT100 [23] (#MN1060, Lot: NE172687, Thermo Fisher Scientific), AT180 [24] (#MN1040, Lot: NJ176312, Thermo Fisher Scientific) and AT270 [25] (#MN1050, Lot: ND169027, Thermo Fisher Scientific). Anti-tau 1 recognizes the non-phosphorylated form of tau at Ser199 and Ser202. Anti-AT8 recognizes tau phosphorylation at Ser202 and Thr205. Therefore a mixture of anti-tau 1 and anti-AT8 is used for detection of total-tau. Anti-AT100 recognizes tau phosphorylation at Ser212 and Thr214. Anti-AT180 recognizes tau phosphorylation at Thr231. AT270 recognizes tau phosphorylation at Thr181. Anti-AT8, -AT100, -AT180 and -AT270 recognize PHF-tau. In addition, an anti-acetylated tubulin mouse monoclonal antibody [26] (#sc-23950, Lot: B0711, Santa Cruz), which indicates tubulin stabilization, was used. In Western blot analysis, a horseradish peroxidase conjugated second antibody (Promega; diluted 1:2000) was used. In immunohistochemistry, Alexa Flour 488-labeled anti-mouse secondary antibodies (Invitrogen; diluted 1:1000) were used against Tau1, AT8, AT100 and AT270. Alexa Fluor 488-labeled anti-rabbit secondary antibodies (Invitrogen; diluted 1:1000) were used against anti-p-tau^{S199,S202} antibodies. Alexa Fluor 568-labeled anti-mouse secondary antibodies (Invitrogen; diluted 1:1000) were used against anti-acetylated tubulin antibodies.

2.3. Molecular cloning of testis tau

Total RNA extraction from the testis was performed using an ISOGEN (Nippon Gene, Tokyo, Japan) and total RNA was stored at −80 °C until use. Poly (A) RNA was isolated using Poly (A) isolation Kit from Total RNA (Nippon Gene, Tokyo, Japan). Specific primers were designed on the basis of the sequences of Tau (forward: caggtcgaagattggctctact, reverse: ctggactctgtccttgaagtcc). The samples were reverse transcribed and cDNA synthesized using Rever Tra Ace (Nacalai Tesque). We acquired 286 bp partial sequence using taq DNA polymerase and following consensus primers obtained from mouse genes to initiate molecular cloning. For 3′RACE, PCR was performed using the gene specific primer 5′-gcc agg agg tgg cca ggt gga ag-3′ and specific adaptor primer (3′-Full RACE core Set, Takara, Kyoto Japan). For 5′RACE, PCR was performed using the gene specific primer, 5′-gct cag gtc cac cgg ctt gta gac-3′ and specific adaptor primer SMARTer RACE cDNA Amplification Kit (Takara, Kyoto, Japan). DNA sequencing was carried out with using the BigDye 3.1 reagent (Applied Biosystems, Tokyo, Japan) and 3130 genetic analyzer (Applied Biosystems, Tokyo, Japan).

2.4. Western blot analysis

Mouse testes ($n = 3$) were removed surgically and stored at −80 °C until use. Tris-Buffered Saline, protease inhibitor and phosphatase inhibitor were added to tissues then homogenized. Sample Buffer Solution with 2-mercaptoethanol (2×) for sodium dodecyl sulfate polyacrylamide gel electrophoresis (Nacalai Tesque, Kyoto, Japan) was added to the homogenized sample then sonicated. After boiling, samples were electrophoresed on polyacrylamide gels and transferred onto Immobilon-P transfer membranes (Millipore). These were incubated with Blocking One (Nacalai Tesque) then incubated with primary antibodies at 4 °C. Bound antibodies were detected by a horseradish peroxidase conjugated second antibody (Promega; diluted 1:2000) using an enhanced Chemi-Lumi One (Nacalai Tesque). Images were obtained with a Fujifilm LAS3000-mini image analysis system (Fujifilm Life Science, Tokyo, Japan) and analyzed with built-in software.

2.5. Immunohistochemistry

Mouse testes were removed surgically, fixed with methacarn (methanol:chloroform:acetic acid = 6:3:1) fixative, embedded in paraffin wax and sectioned. Cross-sections (10 μm) were deparaffinized then incubated with HistoVT One (Nacalai Tesque) at 90 °C for 30 min. After washing, sections were incubated with Blocking One (Nacalai Tesque) at 4 °C for 1 h then incubated with primary antibodies at 4 °C overnight. Immunoreactive elements were visualized with Alexa Fluor 488-labeled anti-rabbit secondary antibodies and Alexa Fluor 568-labeled anti-mouse secondary antibodies (Invitrogen; diluted 1:1000) by treating at 4 °C for 3 h. Nuclei were counterstained with Hoechst 33342 (Molecular Probes; diluted 1:5000). Stained images were obtained with an LSM-700 confocal laser microscope (Carl Zeiss, Oberkochen, Germany) and analyzed with ZEN-2010 software attached to the LSM-700.

3. Results

3.1. Determination of testis tau cDNA sequences

Analysis of tau cDNA sequence expressed in testis revealed that the sequence was confirmed with tau isoform-D (uniprot P10637-5)

3.2. Analysis of expression and phosphorylation pattern in the testis

In the testis, the anti-tau 1 antibody, which recognizes non-phosphorylation at Ser199 and Ser202, detected one major band with apparent molecular mass of 37 kDa and one minor band of 55 kDa in mice at 12 weeks of age (Fig. 1A). Anti-AT8, which recognizes phosphorylation at Ser202 and Thr205, detected several closely spaced bands with molecular masses between 50 and 60 kDa and two bands with apparent molecular mass of 40 and 37 kDa (Fig. 1B). Because detection of the antigen using tau 1 and AT8 antibody are almost complementary, immunohistochemistry using anti-tau 1 antibody and anti-AT8 antibody showed that total-tau protein was detected throughout spermatogenesis (Fig. 1C–E).

3.3. Dynamic changes in phosphorylation status

Immunohistochemistry using anti-AT8, -AT100 and -AT270 antibodies detected phosphorylated tau protein during spermatogenesis. Interestingly, spermatocytes during meiosis intensely stained with AT8, AT100 and AT270 (Fig. 2). AT8 and AT100 were localized all over spermatocytes except around the nucleus (asterisk in Fig. 2A and B). AT270 was detected in whole spermatocytes

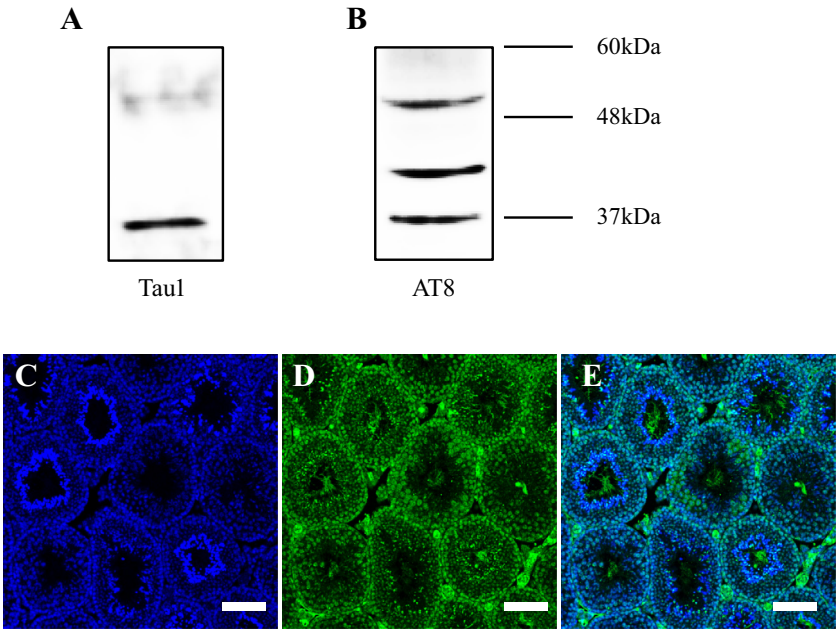

Fig. 1. Western blot analysis of testes from 12-week-old mice ($n = 3$). Tau protein was detected by antibodies against tau 1 (diluted 1:500) (A) and tau 5 (diluted 1:500) (B). Tau 1 detected one major band with molecular mass of 37 kDa and one minor band with molecular mass of 55 kDa (A). AT8 detected several closely spaced bands with molecular masses between 50 and 60 kDa, one major band with apparent molecular mass of 40 kDa and one minor band with apparent molecular mass of 37 kDa (B). Immunohistochemistry of the adult mouse testis. This section and the section in Fig. 3 are serial sections each other. Blue signals represent nuclear DNA counterstained with Hoechst 33342 (diluted 1:5000) (C). Green signals represent total-tau immunostained with anti-tau 1 (diluted 1:20) and anti-AT8 (diluted 1:20) (D). And merged image (E). Scale bar = 100 μm.

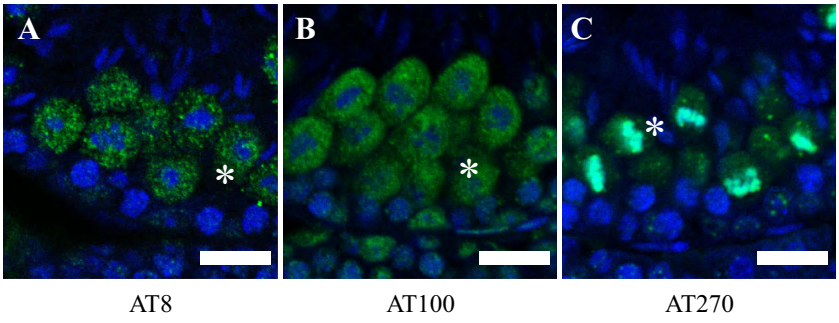

Fig. 2. Immunohistochemistry of the adult mouse testis. Images of seminiferous epithelia at stage XII. Zygotene spermatocytes, spermatocytes during meiotic division (indicated by asterisks) and step 12 elongating spermatids are present. Blue signals represent nuclear DNA counterstained with Hoechst 33342 (diluted 1:5000). Green signals represent immunostaining with anti-AT8 (diluted 1:50) (A), -AT100 (diluted 1:50) (B) and -AT270 (diluted 1:500) (C) antibodies. Scale bars = 20 μm.

and, in contrast to other antibodies, it was detected intensely at the nucleus (asterisk in Fig. 2C). P-tau^{T231} was not detected by anti-AT180 (data not shown).

In order to investigate the effect of tau phosphorylation on tubulin modification, we performed double staining with the anti-p-tau^{S199,S202} antibody and anti-acetylated tubulin antibody on serial sections. P-tau^{S199,S202} antibody detected phosphorylated tau protein during spermatogenesis. P-tau^{S199,S202} was also intensely stained in spermatocytes during meiosis (Fig. 3). Acetylated tubulin was almost not detected in spermatocytes during meiosis (Fig. 3). In order to investigate localization patterns of p-tau^{S199,S202} during spermatogenesis, we classified sections of seminiferous tubules under five stages, stage I, V, VIII, X and XII. Stage classification was based on Staging for Laboratory Mouse [27]. P-tau^{S199,S202} was detected from spermatogonia to step 8 round spermatids (Fig. 4). Spermatocytes during meiosis were intensely stained for p-tau^{S199,S202} (arrows in Fig. 4U–X). Conversely, staining with the anti-acetylated tubulin antibody showed that acetylated tubulin was expressed in spermatogenic cells from diplotene spermatocytes (arrowheads in Fig. 4Q–T) to step 8 round spermatids (asterisks in Fig. 4E–H), but was not detected in spermatocytes during meiosis (arrows in Fig. 4U–X). Double staining with the anti-p-tau^{S199,S202} antibody and anti-acetylated tubulin antibody revealed that the expression of acetylated tubulin decreased as p-tau^{S199,S202} increased. The latter was expressed all over spermatocytes except around the nucleus.

4. Discussion

Tau promotes tubulin assembly in vitro [3] and stabilizes microtubules against depolymerization in vivo [4,5]. An increase in tau phosphorylation reduces its affinity for microtubules, which results in neuronal cytoskeleton destabilization [28]. Conversely, the function of tau protein and its phosphorylation in the testis have not been characterized although its presence has been suggested [9,19].

Western blot analysis showed tau 1 and AT8 detect some bands with apparent molecular masses between 37 and 40 kDa in the

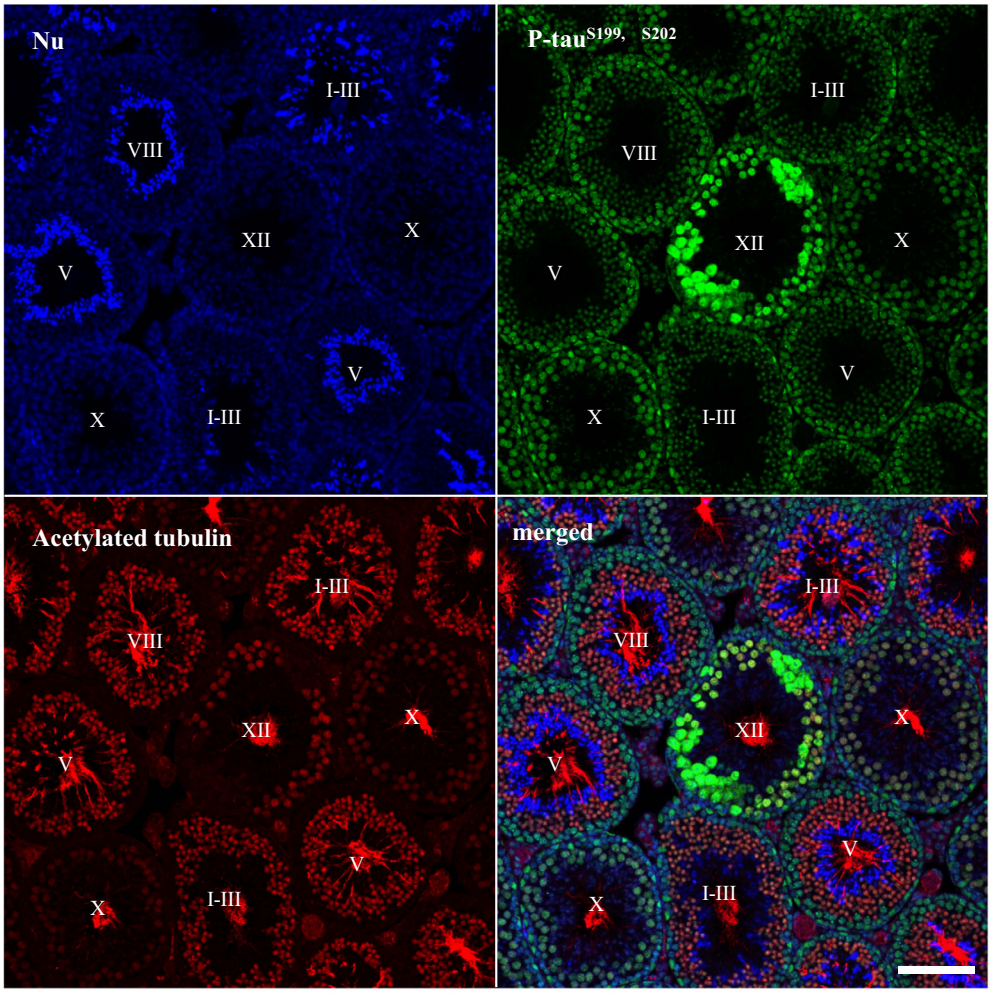

Fig. 3. Immunohistochemistry of adult mouse testis. Blue signals represent DNA counterstaining with Hoechst 33342 (diluted 1:5000). Green signals represent immunostaining for P-tau^{S199,S202} (diluted 1:1000). Red signals represent immunostaining for acetylated tubulin (diluted 1:500). Stages of seminiferous tubules were indicated. Scale bar = 100 μm.

mouse testis (Fig. 1A and B). To date, it has also been reported in the bull and rat [9,19]. In the adult rat brain, alternative splicing of the primary transcript of tau generates six isoforms with an apparent molecular weight between 48 and 67 kDa. However, Gu et al show tau protein was detected in two major bands in the testis with an apparent molecular mass of 34 and 37 kDa after alkaline phosphatase treatment. They suggest this different expression pattern indicates the presence of a testis-specific isoform [9]. In mouse, tau isoform-D (identifier: P10637-5) (uniprot) which molecular weight is about 39 kDa has been discovered [29]. Our sequencing of tau cDNA in the testes ensured that testis tau is corresponding with tau isoform-D. Our Western blot results also demonstrated that the presence of total tau protein with apparent molecular masses of 37 kDa in adult mice (Fig. 1A and B), consistent with previous reports. Furthermore, immunohistochemistry was performed to investigate the localization of phosphorylated tau.

PHFs are composed of highly phosphorylated tau and accumulate in the brain of subjects with AD [30,31]. To elucidate the localization of site-specific phosphorylation status, several antibodies against p-tau were used. The anti-AT8, -AT100 and -AT270 antibodies recognize PHF-tau. Immunohistochemical studies indicated not only tau expression but also its phosphorylation patterns in the testis. Although total-tau expression, detected by anti-tau 1 and anti-AT8 and non-phosphorylated tau at S199, S202, detected by anti-tau 1, were constantly observed from spermatogonia to round spermatids (Fig. 1C–E, S1), p-tau^{S199,S202}, AT8, AT100 and AT270 were especially localized in spermatocytes during meiosis (Fig. 2–4). These results suggested that tau expression was not specific during meiosis but the phosphorylation is specific. In addition, because these antibodies specifically detected the phosphorylation in meiosis, we suggest that Tau might be phosphorylated at AD-specific sites in meiosis. Interestingly, the period of tubulin deacetylation was coincident with that of tau phosphorylation at the time of meiosis (Fig. 4A–D, U–X). The relationship between tau phosphorylation and tubulin acetylation is unidentified. However, North and Verdin reported that activity of the microtubule deacetylase, SIRT2, was elevated during mitotic division, suggesting its involvement in destabilization of the spindle microtubule for chromosome movements [32]. On the other hand, tau acts as HDAC6 inhibitor and PHFs exert the stronger inhibiting actions than tau [33]. During spermatogenesis, the expression level of HDAC6 was high in spermatogonia and low from pachytene spermatocytes to elongating spermatids [34]. Therefore, these site-specific phosphorylation localizations suggest involvement of spindle microtubule destabilization during meiotic division. Further studies are necessary to clarify the relation between tau and microtubule deacetylases.

Chromosomal segregation in both mitotic and meiotic division is controlled by spindle microtubule elongation and retraction.

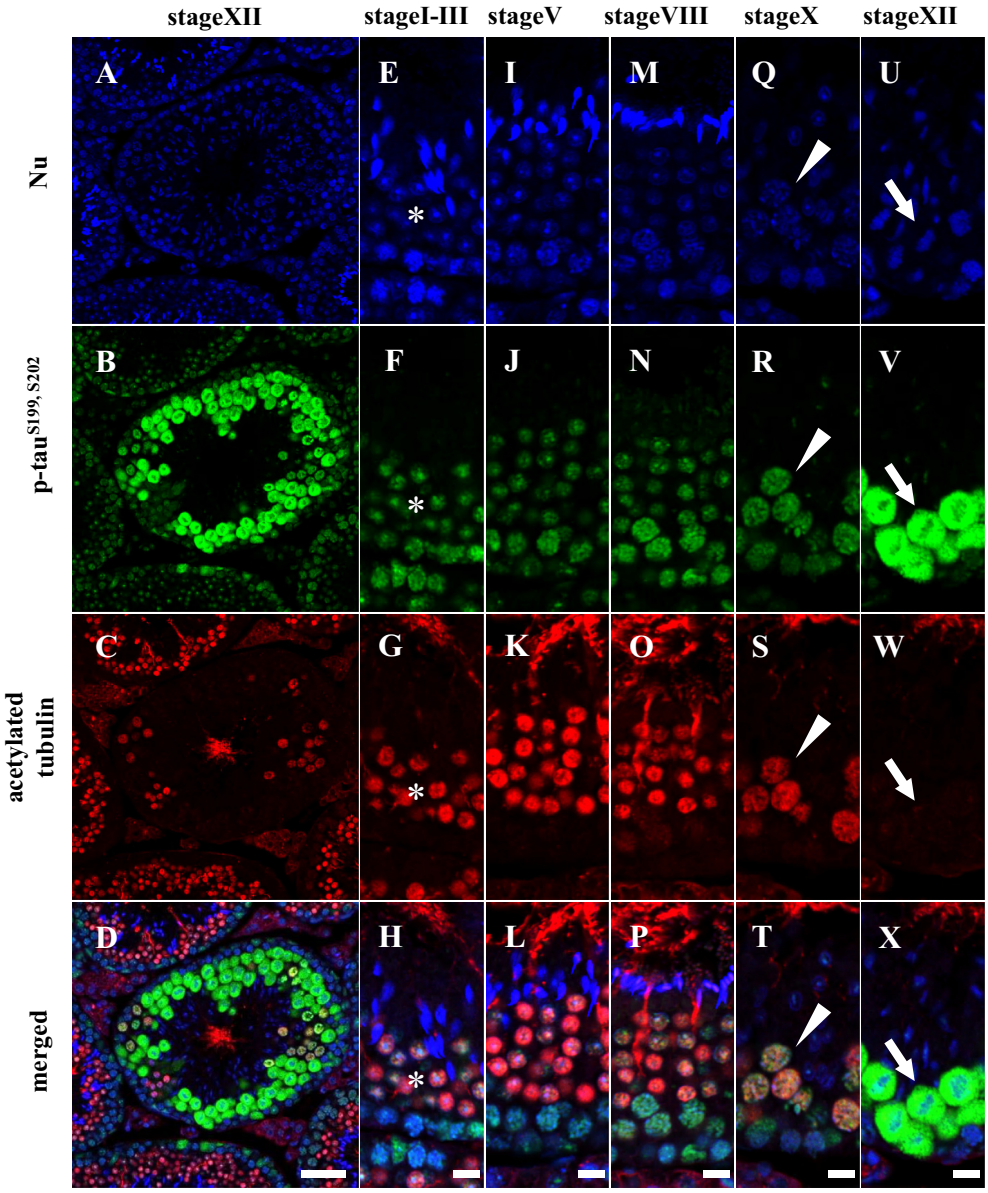

Fig. 4. Immunohistochemistry of adult mouse testis. (A, E, I, M, Q, U) Blue signals represent DNA counterstaining with Hoechst 33342 (diluted 1:5000). (B, F, J, N, R, V) Green signals represent immunostaining for P-tau^{S199,S202} (diluted 1:1000). (C, G, K, O, S, W) Red signals represent immunostaining for acetylated tubulin (diluted 1:500). (D, H, L, P, T, X) Merged Images. (A–D) Images of seminiferous tubules at stage XII. (E–X) Images of seminiferous epithelia. (E–H) Seminiferous epithelia at stages I–III. Early pachytene spermatocytes, step 1 round spermatids (asterisks) and step 13 elongated spermatids are present. (I–L) Seminiferous epithelium at stage V. Intermediate spermatogonia, pachytene spermatocytes, step 5 round spermatids and step 15 elongated spermatids are present. (M–P) Seminiferous epithelium at stage VIII. Preleptotene spermatocytes, pachytene spermatocytes, step 7 round spermatids and step 16 elongated spermatids are present. (Q–T) Seminiferous epithelium at stage X. Leptotene spermatocytes, late pachytene spermatocytes (indicated by arrowheads) and step 10 elongating spermatids are present. (U–X) Seminiferous epithelium at stage XII. Zygotene spermatocytes, spermatocytes during meiotic division (arrows) and step 12 elongating spermatids are present. (A–D) Scale bars in A–D = 50 μm; scale bars in E–X = 10 μm.

Segregation errors during meiotic division cause chromosomal aberrations, which if transferred to offspring cause malformation and miscarriage. Spindles, mainly composed of microtubules, are controlled by MAPs. It is known that spindle microtubules repeatedly extend and retract to catch the kinetochores of chromosomes during metaphase of mitotic and meiotic divisions [35,36]. Therefore, phosphorylation of the protein might contribute to this extension and retraction of microtubules during meiotic division.

Futhermore, the relationship between tau and DNA/chromosomes has recently reported. Tau has been reported to protect DNA from Oxidation and heat stresses [37,38]. In this study, P-tau^{S202,T205} and P-tau^{S212,T214} are localized all over spermatocytes except around the nucleus (Fig. 2A and B). This result agrees with the previous report [38]. In addition, P-tau^{T181} is localized at the nucleus (Fig. 2C). These results suggest that tau may interact with DNA/chromosomes also in the testis.

In conclusion, we have revealed that site-specific tau phosphorylation is localized specifically during spermatogenesis. Furthermore, there appears to be an interaction between tau phosphorylation and microtubule deacetylation, suggesting the possibility of involvement of both processes during meiosis.

Appendix A. Supplementary data

Supplementary data associated with this article can be found, in the online version, at http://dx.doi.org/10.1016/j.febslet.2014.04.021.

References

[1] Neely, M.D. and Boekelheide, K. (1988) Sertoli cell processes have axoplasmic features: an ordered microtubule distribution and an abundant high molecular weight microtubule-associated protein (cytoplasmic dynein). J. Cell Biol. 107, 1767–1776.

[2] Cleveland, D.W., Hwo, S.Y. and Kirschner, M.W. (1977) Physical and chemical properties of purified tau factor and the role of tau in microtubule assembly. J. Mol. Biol. 116, 227–247.

[3] Weingarten, M.D., Lockwood, A.H., Hwo, S.Y. and Kirschner, M.W. (1975) A protein factor essential for microtubule assembly. Proc. Natl. Acad. Sci. U.S.A. 72, 1858–1862.

[4] Drubin, D.G. and Kirschner, M.W. (1986) Tau protein function in living cells. J. Cell Biol. 103, 2739–2746.

[5] Kanai, Y., Takemura, R., Oshima, T., Mori, H., Ihara, Y., Yanagisawa, M., Masaki, T. and Hirokawa, N. (1989) Expression of multiple tau isoforms and microtubule bundle formation in fibroblasts transfected with a single tau cDNA. J. Cell Biol. 109, 1173–1184.

[6] Yoshida, H. and Ihara, Y. (1993) Tau in paired helical filaments is functionally distinct from fetal tau: assembly incompetence of paired helical filament-tau. J. Neurochem. 61, 1183–1186.

[7] Goedert, M., Spillantini, M.G., Jakes, R., Rutherford, D. and Crowther, R.A. (1989) Multiple isoforms of human microtubule-associated protein tau: sequences and localization in neurofibrillary tangles of Alzheimer's disease. Neuron 3, 519–526.

[8] Goedert, M., Spillantini, M.G., Potier, M.C., Ulrich, J. and Crowther, R.A. (1989) Cloning and sequencing of the cDNA encoding an isoform of microtubule-associated protein tau containing four tandem repeats: differential expression of tau protein mRNAs in human brain. EMBO J. 8, 393–399.

[9] Gu, Y., Oyama, F. and Ihara, Y. (1996) Tau is widely expressed in rat tissues. J. Neurochem. 67, 1235–1244.

[10] Buee, L., Bussiere, T., Buee-Scherrer, V., Delacourte, A. and Hof, P.R. (2000) Tau protein isoforms, phosphorylation and role in neurodegenerative disorders. Brain Res. Brain Res. Rev. 33, 95–130.

[11] Hanger, D.P., Betts, J.C., Loviny, T.L., Blackstock, W.P. and Anderton, B.H. (1998) New phosphorylation sites identified in hyperphosphorylated tau (paired helical filament-tau) from Alzheimer's disease brain using nanoelectrospray mass spectrometry. J. Neurochem. 71, 2465–2476.

[12] Sergeant, N. et al. (2008) Biochemistry of Tau in Alzheimer's disease and related neurological disorders. Expert Rev. Proteomics 5, 207–224.

[13] Dickey, C.A. et al. (2007) The high-affinity HSP90-CHIP complex recognizes and selectively degrades phosphorylated tau client proteins. J. Clin. Invest. 117, 648–658.

[14] Drewes, G., Trinczek, B., Illenberger, S., Biernat, J., Schmitt-Ulms, G., Meyer, H.E., Mandelkow, E.M. and Mandelkow, E. (1995) Microtubule-associated protein/microtubule affinity-regulating kinase (p110mark). A novel protein kinase that regulates tau-microtubule interactions and dynamic instability by phosphorylation at the Alzheimer-specific site serine 262. J. Biol. Chem. 270, 7679–7688.

[15] Sengupta, A., Kabat, J., Novak, M., Wu, Q., Grundke-Iqbal, I. and Iqbal, K. (1998) Phosphorylation of tau at both Thr 231 and Ser 262 is required for maximal inhibition of its binding to microtubules. Arch. Biochem. Biophys. 357, 299–309.

[16] Ishiguro, K. et al. (1999) Phosphorylated tau in human cerebrospinal fluid is a diagnostic marker for Alzheimer's disease. Neurosci. Lett. 270, 91–94.

[17] Itoh, N. et al. (2001) Large-scale, multicenter study of cerebrospinal fluid tau protein phosphorylated at serine 199 for the antemortem diagnosis of Alzheimer's disease. Ann. Neurol. 50, 150–156.

[18] Hampel, H. et al. (2004) Measurement of phosphorylated tau epitopes in the differential diagnosis of Alzheimer disease: a comparative cerebrospinal fluid study. Arch. Gen. Psychiatry 61, 95–102.

[19] Ashman, J.B., Hall, E.S., Eveleth, J. and Boekelheide, K. (1992) Tau, the neuronal heat-stable microtubule-associated protein, is also present in the cross-linked microtubule network of the testicular spermatid manchette. Biol. Reprod. 46, 120–129.

[20] Kishi, M., Pan, Y.A., Crump, J.G. and Sanes, J.R. (2005) Mammalian SAD kinases are required for neuronal polarization. Science 307, 929–932.

[21] Lee, D.C. et al. (2010) LPS-induced inflammation exacerbates phospho-tau pathology in rTg4510 mice. J. Neuroinflammation 7, 56.

[22] Goedert, M., Jakes, R., Crowther, R.A., Cohen, P., Vanmechelen, E., Vandermeeren, M. and Cras, P. (1994) Epitope mapping of monoclonal antibodies to the paired helical filaments of Alzheimer's disease: identification of phosphorylation sites in tau protein. Biochem. J. 301 (Pt 3), 871–877.

[23] Mailliot, C., Bussiere, T., Caillet-Boudin, M.L., Delacourte, A. and Buee, L. (1998) Alzheimer-specific epitope of AT100 in transfected cell lines with tau: toward an efficient cell model of tau abnormal phosphorylation. Neurosci. Lett. 255, 13–16.

[24] Ho, Y.S. et al. (2012) Endoplasmic reticulum stress induces tau pathology and forms a vicious cycle: implication in Alzheimer's disease pathogenesis. J. Alzheimers Dis. 28, 839–854.

[25] Brecht, W.J. et al. (2004) Neuron-specific apolipoprotein e4 proteolysis is associated with increased tau phosphorylation in brains of transgenic mice. J. Neurosci. 24, 2527–2534.

[26] Wilson, C.H. and Christie, A.E. (2010) Distribution of C-type allatostatin (C-AST)-like immunoreactivity in the central nervous system of the copepod *Calanus finmarchicus*. Gen. Comp. Endocrinol. 167, 252–260.

[27] Russell, L.D. et al. (1990) Histological and Histopathological Evaluation of the Testis, Cache River Press. Chapter 4 Staging for Laboratory Species, pp. 119–21.

[28] Grundke-Iqbal, I., Iqbal, K., Tung, Y.C., Quinlan, M., Wisniewski, H.M. and Binder, L.I. (1986) Abnormal phosphorylation of the microtubule-associated protein tau (tau) in Alzheimer cytoskeletal pathology. Proc. Natl. Acad. Sci. U.S.A. 83, 4913–4917.

[29] Kenner, L. et al. (1994) Expression of three- and four-repeat tau isoforms in mouse liver. Hepatology 20, 1086–1089.

[30] Lee, V.M., Balin, B.J., Otvos Jr., L. and Trojanowski, J.Q. (1991) A68: a major subunit of paired helical filaments and derivatized forms of normal Tau. Science 251, 675–678.

[31] Goedert, M. (1993) Tau protein and the neurofibrillary pathology of Alzheimer's disease. Trends Neurosci. 16, 460–465.

[32] North, B.J. and Verdin, E. (2007) Interphase nucleo-cytoplasmic shuttling and localization of SIRT2 during mitosis. PLoS ONE 2, e784.

[33] Perez, M. et al. (2009) Tau – an inhibitor of deacetylase HDAC6 function. J. Neurochem. 109, 1756–1766.

[34] Hazzouri, M., Pivot-Pajot, C., Faure, A.K., Usson, Y., Pelletier, R., Sele, B., Khochbin, S. and Rousseaux, S. (2000) Regulated hyperacetylation of core histones during mouse spermatogenesis: involvement of histone deacetylases. Eur. J. Cell Biol. 79, 950–960.

[35] Walczak, C.E. and Heald, R. (2008) Mechanisms of mitotic spindle assembly and function. Int. Rev. Cytol. 265, 111–158.

[36] Kitajima, T.S., Ohsugi, M. and Ellenberg, J. (2011) Complete kinetochore tracking reveals error-prone homologous chromosome biorientation in mammalian oocytes. Cell 146, 568–581.

[37] Wei, Y., Qu, M.H., Wang, X.S., Chen, L., Wang, D.L., Liu, Y., Hua, Q. and He, R.Q. (2008) Binding to the minor groove of the double-strand, tau protein prevents DNA from damage by peroxidation. PLoS ONE 3, e2600.

[38] Sultan, A. et al. (2011) Nuclear tau, a key player in neuronal DNA protection. J. Biol. Chem. 286, 4566–4575.